Published in final edited form as:
Nanotoxicology. 2014 February ; 8(1): 17–27. doi:10.3109/17435390.2012.744110.

IL-1R signalling is critical for regulation of multi-walled carbon nanotubes-induced acute lung inflammation in C57Bl/6 mice

Teri Alyn Girtsman[1], **Celine A Beamer**[1], **Nianqiang Wu**[2], **Mary Buford**[1], and **Andrij Holian**[1]

[1]University of Montana, Department of Biomedical and Pharmaceutical Sciences, Center for Environmental Sciences, 32 Campus Drive, Missoula, MT, USA

[2]West Virginia University, Department of Mechanical & Aerospace Engineering, P.O. Box 6106, Morgantown, WV, USA

Abstract

Exposure to certain engineered nanomaterials has been associated with pathological changes in animal models raising concerns about potential human health effects. MWCNT have been reported to activate the NLRP3 inflammasome *in vitro*, correlating with lung inflammation and pathology, *in vivo*. In this study, we investigated the role of IL-1 signalling in pulmonary inflammatory responses in WT and IL-1R−/− mice after exposure to MWCNT. The results suggest that MWCNT were effective in inducing acute pulmonary inflammation. Additionally, WT mice demonstrated significant increased airway resistance 24 h post exposure to MWCNT, which was also blocked in the IL-1R−/− mice. In contrast, by 28 days post exposure to MWCNT, the inflammatory response that was initially absent in IL-1R−/− mice was elevated in comparison to the WT mice. These data suggest that IL-1R signalling plays a crucial role in the regulation of MWCNT-induced pulmonary inflammation.

Keywords

nanotubes; nanotoxicology; environmental toxicology; particle characterisation

Introduction

Engineered nanomaterials (ENM) are a large variety of particles with at least one dimension in the 1–100 nm range. Multi-walled carbon nanotubes (MWCNT), in particular, possess properties, such as high surface area and tensile strength, that make them very attractive for technological and biomedical product development (Harris 1999; Martin & Kohli 2003). Results from studies assessing the safety of ENM indicate that significant lung pathologies can arise following exposure to these materials (Johnston et al. 2010). For example, MWCNT have been shown to provoke allergic, inflammatory and fibrotic pulmonary

Correspondence: Teri Alyn Girtsman, University of Montana, Biomedical and Pharmaceutical Sciences, Center for Environmental Sciences, 32 Campus Drive, Missoula, 59812, USA. tag329@gmail.com.

Declaration of interest
The authors report no conflicts of interest. The authors alone are responsible for the content and writing of the paper.

responses in animal models (Inoue et al. 2009). Although there is intense interest in describing the mechanisms by which some ENM (including MWCNT) cause inflammation and injury, the underlying mechanism(s) to explain the bioactivities of ENM remain unclear.

Innate immune defences in the lung are primarily responsible for the clearance of particles deposited in the respiratory tract. More than any other cytokine family, the IL-1 family of ligands and receptors are essential to the innate inflammatory response, which includes 11 members coded by 9 distinct genes (Dinarello 2011). IL-1β and, another IL-1 family member, IL-18 are potent pro-inflammatory cytokines that promote an array of innate immune processes (Dolinay et al. 2012; Kang et al. 2012; Dinarello 2009). Both IL-1β and IL18 are initially produced as an inactive cytosolic precursor that requires proteolytic cleavage by caspase-1 for activation and secretion. Activation of caspase-1 occurs following formation of the NLRP3 inflammasome assembly, a large multimeric protein complex that is formed in response to stimulation of macrophages by pathogen-associated molecular patterns (PAMPs). Activation of the NLRP3 inflammasome is initiated by a diverse and growing list of endogenous and exogenous agonists (Davis et al. 2011).

The IL-1 family of receptors also includes decoy receptors, binding proteins and inhibitory receptors (Dinarello 2009). When bound to either IL-1α or IL-1β, the IL-1 receptor (IL-1 ligand-binding chain – IL1RI) recruits and forms a complex with the IL-1 receptor accessory protein (IL1RAcP). Signalling is initiated with recruitment of the adaptor protein MyD88 to the Toll-IL-1 receptor (Medzhitov et al. 1998; Muzio et al. 1997) domain resulting in NF-κB translocating to the nucleus where expression of a large collection of inflammatory genes takes place leading to a cascade of inflammatory events (Weber et al. 2010).

IL-1R signalling has been associated with what has been termed ‘sterile’ immune responses (Rock et al. 2010) from exposure to inhaled particulate matter, diesel exhaust, silica and asbestos, which induce production of IL-1β in the lung (Dostert et al. 2008; Provoost et al. 2011). Furthermore, to emphasise the importance of IL-1β, experiments using IL-1R knockout ($IL\text{-}1R^{-/-}$) mice showed reduced pulmonary inflammatory responses in response to these particles (Churg et al. 2009; Hornung et al. 2008; Provoost et al. 2011). In addition, activation of NLRP3 inflammasome and IL-1β production has been linked to the induction of pulmonary fibrosis (Dostert et al. 2008).

Recent studies have demonstrated that ENM induced cell toxicity, oxidant stress, cytokine production, lysosomal disruption and NLRP3 inflammasome activation (Hamilton et al. 2009; Liu et al. 2007; Nel et al. 2006). *In vitro* analysis of MWCNT using peripheral blood mononuclear and THP-1 cells has demonstrated that MWCNT increase IL-1β production (Murphy et al. 2012; Palomaki et al. 2011). Furthermore, Porter et al. have recently published the first study demonstrating induction IL-1β release through NLRP3 inflammasome activation by titanium dioxide nanospheres and nanobelts *in vivo* (Murphy et al. 2012; Palomaki et al. 2011; Porter et al. 2012). Furthermore, our studies have shown a good correlation between the ability of a metal oxide (i.e., TiO_2) and MWCNT to activate the NLRP3 inflammasome using murine primary alveolar macrophages (AM) (Hamilton et al. 2012a). However, the precise role of NLRP3 inflammasome-related cytokines has not been established in the inflammatory and fibrotic responses to MWCNT.

The MWCNT used in this study were selected from a collection of 24 commercially available and characterised MWCNT procured and provided to us by the National Toxicology Program. Our analysis of the metal impurities in these particles revealed that only the Ni content was associated with increased activation of the NLRP3 inflammasome (Hamilton et al. 2012b). To this end, the two selected MWCNT were 1) 'low-nickel' LN-MWCNT and 2) 'high-nickel' HN-MWCNT (see Table I). These particles were selected to investigate the MWCNT-induced pulmonary inflammatory response based on prior *in vitro* analysis demonstrating an increased toxicity and bioactivity associated with increased nickel impurity (LN-MWCNT are 2.54% and HN-MWCNT are 5.54% – percentage of total particle mass), and the level of inflammasome activation. In addition, other studies have indicated that nickel contributes to the bioactivity of single-walled carbon nanotubes (Liu et al. 2007). In this study, we examined the role of NLRP3 inflammasome-generated IL-1β signalling in the pulmonary inflammatory response in C57BL/6 mice, induced by MWCNT. The role of IL-1β was examined using IL-1RI null mice compared to wild-type mice. Acute and chronic inflammatory responses were monitored, as well as airway hyperreactivity and lung injury (pathology).

Methods

Characterisation of multi-walled carbon nanotubes

The bulk MWCNT samples were provided by Dr. Nigel Walker and Brad Collins at the National Toxicology Program (NTP) at the National Institute of Environmental Health Sciences (NIEHS). Procurement and characterisation of the bulk unformulated MWCNT were carried out for the NTP by the Research Triangle Institute under NIEHS contract N01-ES-65554.

Vendor addresses

Low Ni-MWCNT (FA-04):MK Impex Corp, Mississauga, ON, Canada; www.mknano.com. High Ni-MWCNT (FA-21): Sun Innovations Sun Innovations, Inc., Fremont, CA, USA; www.nanomaterialstore.com.

Purity of each MWCNT was analysed by thermogravimetric analysis. A TGA Q500 Thermogravimetric Analyzer (TA Instruments, New Castle, DE) was used for the analysis. A nominal 10 mg aliquot of each sample was accurately weighed and transferred to a platinum sample pan and then the TGA for analysis. The instrument was gradually ramped to a temperature of 850°C. Duplicate aliquots of each study sample were analysed. Metal content of each of the MWCNT study samples was determined by X-ray fluorescence (XRF) spectrometry. A nominal 250 mg aliquot of each sample was transferred to an XRF sample cup and sealed with film. Cups were loaded into the ThermoNoran Quant'X energy dispersive XRF (now listed as ThermoFisher, Pittsburgh, PA) and were analysed with filter conditions optimised for determination of Fe, Co, Ni, Mo and Y. Using these filter conditions, the presence of additional metals present at significant levels have been detected. Samples were analysed in duplicate. An FEI Tecnai G^2 Twin Transmission Electron Microscope (FEI Tecnai, Hillsborough, OR) (Shared Materials Instrumentation Facility, Duke University) with an ultrathin carbon type-A, 400 Mesh copper TEM Grid (Ted Pella,

Inc., Redding, CA) was used to determine the diameter of the MWCNT samples. Over 50 representative TEM images were taken and an average of >150 MWCNT was measured for each sample. Fovea Pro software (Beirut, Lebanon) was used for the diameter measurement. The procedure involves threshold adjustment and MWCNT overlap area masking to obtain accurate measurement of the MWCNT diameters. Dynamic light scattering was used to measure agglomerate size and the Malvern Zetasizer Nano ZS (Malvern, Worcestershire, UK) instrument to determine the zeta potential of each MWCNT.

In vivo mouse exposures

Instillation—Wild-type C57BL/6 and IL-1R$^{-/-}$ mice (2 months old) were obtained from Jackson Laboratories (Bar Harbor, ME) and were housed in controlled environmental conditions (22 ± 2°C; 30–40% humidity, 12-h light: 12-h dark cycle) and provided food and water *ad libitum*. All procedures were performed under protocols approved by the IACUC (036-09AHCEHS-071409) All nanoparticles were suspended (1.67 mg/ml) in dispersion medium (Porter et al. 2008) (PBS containing 0.6 mg/ml mouse serumalbumin (Sigma-Aldrich, Saint Louis, MO) and 0.01 mg/ml 1,2-dipalmitoyl-sn-glycero-3-phosphocholine (Sigma-Aldrich) and suspended using a cup-horn sonication for 1 min. Mice were exposed to nanoparticles by oral pharyngeal aspiration (Foster et al. 2001; Lacher et al. 2010). Briefly, the mice were anaesthetised using inhalation isoflurane and a volume of 30 μl of particle suspension (50 μg) was delivered into the back of the throat. By holding the tongue to the side, the solution was aspirated into the lungs.

Whole lung lavage (WLL)—Mice were euthanised with sodium pentobarbital (Euthasol™). The lungs and trachea were exposed by thoracotomy. The trachea was cannulated with a blunted 25 g needle. One ml of ice cold PBS (pH 7.4) was injected into the lungs and immediately withdrawn (first pull), which was followed by four additional repeats. Lung lavage cells were collected by centrifugation (400 × *g*, 5 min, 4°C) and cell counts obtained using a Coulter Z2 particle counter (Beckman Coulter, Brea, CA). The cells were pooled while the first pull of whole lung lavage fluid (WLLF) was stored at −20° for cytokine analysis.

Pulmonary function testing—Transpulmonary resistance was assessed as previously described (Wells et al. 2010). Mice were challenged with vehicle (PBS), followed by increasing concentrations of methacholine (1.5, 3, 6, 12 and 24 mg/ml). Aerosols were generated with an ultrasonic nebulizer (Aeroneb Laboratory Nebulizer; Buxco Electronics, Inc., Troy, NY). A computer programme (FinePointe Software; Buxco Electronics) was used to calculate R_L.

Histology—Blood was perfused from the lungs of each mouse followed by inflation-fixing through the trachea with 4% paraformaldehyde-PBS and submerged in the same fixative overnight at 4°C. The lungs were washed with cold PBS, dehydrated and embedded in paraffin. Tissue sections (7 μm) were mounted on Superfrost slides (VSR International, Westchester, PA) and stained with Gomori's Trichrome (EMD Chemicals, Gibbstown, NJ) for histological analysis using a Thermo Shandon automated stainer (Shandon, Pittsburgh, PA).

Cytokine assays—Mouse cytokine and chemokine kits: IL-1β, IL-6, TNFα and MCP-1 DuoSets were obtained from R&D Systems and ELISA assays were performed according to the manufacturer's protocol. The cytokine levels in WLLF were quantified at 450 nm using a SpectraMax 190 automated plate reader (Thermo Scientific, West Palm Beach, FL) at 495 nm. The data were analysed using Softmax Pro software (Thermo Scientific).

Hydroxyproline assay

Total collagen of the left lung lobe from 28 day-treated mice was quantified by analysis of hydroxyproline, an amino acid unique to collagen. Briefly, lung tissue from the left lobe was excised, weighed and frozen immediately in liquid nitrogen. The lung tissue was homogenised using a Tissue Tearor in sterile water. An aliquot of lung homogenate was hydrolysed in 12 N HCl at 110°C for 24 h. The mixture was reacted with chloramine T and Ehrlich's reagent to produce a hydroxyproline-chromophore that was quantified a SpectraMax 190 automated plate reader at 550 nm. Hydroxyproline content for each lobe was determined by triplicate analysis of the sample to provide a mean value.

Bright field microscopy—Differential cell counts and mouse lung tissue sections were imaged at 100× using an upright Nikon E-800 (Melville, NY) with bright field, DIC and fluorescence capabilities. Digital images are generated with a Cambridge Research Instrumentation/Nuance multispectral camera. The Nuance camera collects wavelengths in the 420–720 nm range, and the software spectrally classifies and unmixes overlapping dyes.

Scanning electron microscopy (SEM)—Dry nanoparticle samples were placed on a conductive sticky carbon tab on a 12 mm aluminium SEM stub. The stubs were placed, uncoated, in a Hitachi S-4700 Field Emission Scanning Electron Microscope and imaged at 10 kv.

Eosinophil peroxidase assay—Eosinophil peroxidase (EPO) activity in WLL cells was determined by colorimetric assay. WLL cells were centrifuged and suspended in 200 μl of sterile PBS. 100 μl of the cell suspension was added to 100 μl of PBS in a 96-well microtiter plate. The cells were serially titrated to a final dilution of to 1:256. 100 μl of EPO substrate solution, comprised of 0.1 mM orthophenylene diamine dihydrochloride (Sigma-Aldrich) in 50 mM Tris-HCl (Sigma-Aldrich) containing 0.1% Triton X-100 (Sigma-Aldrich) and 1 mM hydrogen peroxide (Sigma-Aldrich) was added to each well. The plate was incubated at room temperature for 10–15 min and 2 N H_2SO_4 was added to stop the reaction. The optical density was determined by reading the plate at 495 nm using a SpectraMax 190 automated plate reader (Thermo Scientific).

Statistical analyses

Two-way ANOVA tests with Tukey *post-hoc* analysis were performed, unless otherwise stated, to evaluate statistical significance. Statistical significance is a probability of type I error at less than 5% ($p < 0.05$). The minimum number of experimental replications was three. Graphics and analyses were performed on PRISM 5.0.

Results

MWCNT characterisation

Characterisation (tube dimensions and extent of catalyst impurities) of the bulk unformulated MWCNT was carried out for the NTP by the Research Triangle Institute and is described in detail in the Methods. Dynamic light scattering studies of LN-or HN-MWCNT suspended in DM revealed that the average agglomerate was 682 nm and 429 nm in average size, respectively. The zeta potentials were −11.3 and −12 mV for LN-and HN-MWCNT, respectively. In addition, HN-MWCNT suspended agglomerates demonstrated bimodal diameter distribution exhibiting peaks at ~145 nm and ~690 nm (Table I). The scanning electron micrographs show the tangled structures of LN- and HN-MWCNT to contain numerous random bends and kinks (Figure 1).

MWCNT induce acute pulmonary inflammation

To assess the inflammatory potential of MWCNT exposure, WLL was collected from C57Bl/6 mice and IL-1 receptor null mice instilled with 50 μg LN- or HN-MWCNT, 24 h post exposure. The dosage was established and selected based on the lowest amount of MWCNT able to reproducibly induce measureable levels of IL-1β and lung fibrosis *in vivo*. Total cell counts from WLL demonstrated elevated cell numbers in WT mice treated with LN- or HN-MWCNT compared to DM-treated control mice indicative of an acute inflammatory response. Although the IL-1R$^{-/-}$ mice treated with HN-MWCNT had an overall increase in total cells that was significant compared to the DM-treated mice, the increase was much less than in the wild-type mice (Figure 2A). Differential cell counts demonstrated significant pulmonary inflammation, with infiltration by several cell types. The data shown in Figure 2B demonstrate that neutrophils and eosinophils were a significant proportion of the influx of inflammatory cells in the lungs of WT mice treated with LN- or HN-MWCNT. The recruitment of both PMNs and eosinophils to the airways of the LN- or HN-MWCNT-treated WT mice were diminished in the IL-1R$^{-/-}$ mice. Particle uptake (observed by light microscopy) in both WT and IL-1R$^{-/-}$ AM demonstrated that IL-1R$^{-/-}$ mice AM were able to take up particles similar to that of WT AM, suggesting that the decreased inflammatory response observed in these mice was not due to an inability of the IL-R$^{-/-}$ AM to respond or uptake particles, but rather to loss of IL-1β signalling (Figure 2C). In addition, the wild-type mice showed that the neutrophilia was greater following HN-MWCNT compared to LN-MWNCT, which was dramatically diminished in the IL-1R$^{-/-}$ mice.

MWCNT induce pro-inflammatory mediators in WLL fluid

To determine the role of IL-1 receptor signalling associated with the inflammatory response, WT and IL-1R$^{-/-}$ mice were instilled with vehicle, LN- or HN-MWCNT then cytokines and chemokines were measured in WLL at 24 h post exposure. Analysis of cytokine and chemotactic factors secreted into the lavage fluid revealed that WT mice respond to both LN- and HN-MWCNT with enhanced secretion of proinflammatory cytokines IL-1β, TNFα and IL-6, as well as the chemokine MCP-1. The response of IL-1R$^{-/-}$ mice to LN-or HN-MWCNT also showed elevated levels of IL-1β, IL-6 and TNFα in the whole lung lavage. However, levels of the chemokine MCP-1 were diminished in the lavage fluid from both

LN- and HN-MWCNT-treated IL-1R$^{-/-}$ mice as compared to WT mice (Figure 3). Although not always significant, there tended to be increased levels of these inflammatory cytokines in the WLL in the HN-MWCNT compared to LN-MWCNT. These findings suggest that the release of MCP-1 was downstream of IL-1β.

MWCNT-induced collagen deposition and granuloma formation

To investigate the contribution of IL-1 receptor signalling in the development of pulmonary fibrosis, lung sections were evaluated from WT or IL-1R$^{-/-}$ mice at 7 and 28 days post exposure to DM, LN- or HN-MWCNT. Trichrome-stained lung tissues of IL-1R$^{-/-}$ mice revealed increased collagen deposition as well as peri-bronchial and peri-vascular inflammation 7 days post HN-MWCNT compared to DM or LN-MWCNT-exposed mice (Figure 4A). Furthermore, progressive collagen deposition was observed in the tissue sections from lungs of IL-1R$^{-/-}$ mice 28 days post exposure compared to the tissues of the 7 day-exposed mice. However, the collagen deposition was not appreciably augmented in the WT mice at 28 days compared to the 7 day-exposed mice. Hydroxyproline quantification within the lung tissue confirmed that there was a slight increase in collagen in HN-MWCNT-treated WT mice that was significantly elevated in the IL-1R$^{-/-}$-exposed mice compared to vehicle controls at 28 days (Figure 4B). Taken together, these findings indicate that in contrast to the 24 h results, where there were minimal changes in the IL-1R$^{-/-}$ mice, the pathology was much worse by 28 days in the IL-1R$^{-/-}$ mice compared to the WT.

MWCNT induce changes in pulmonary function

To determine the acute and chronic effects of MWCNT and IL-1R signalling on pulmonary function, we assessed pulmonary function in WT and IL-1R$^{-/-}$ mice following instillation of DM or HN-MWCNT (these studies focused on the high Ni-MWCNT because of the expected greater effects) at 24 h and 28 days post exposure. The results shown in Figure 5 demonstrate that after 24 h the WT mice responded to methacholine challenge with enhanced airway hyperreactivity, shown by increased lung resistance. In contrast, the IL-1R$^{-/-}$ mice had a diminished acute response to HN-MWCNT compared to WT, demonstrated by the lack of increased R_L to methacholine challenge. These findings support the notion that inflammasome activation and IL-1β signalling are important in the acute physiological response to MWCNT.

Airway hyperreactivity was also assessed in WT and IL-1R$^{-/-}$ mice 28 days after exposure to a single installation of HN-MWCNT to determine whether chronic effects were similar to the acute. In contrast to the acute outcome, at 28 days the IL-1R null mice had a marked increased R_L to methacholine, whereas the response appeared to resolve in the WT mice with no observable difference between the particle and DM-treated mice in R_L (Figure 5). Therefore, it appears that IL-1R signalling is involved both in the acute inflammatory responses as well as the resolution phase of inflammation.

Ni-MWCNT induces acute airway eosinophilia in WT mice that was diminished in IL-1R$^{-/-}$ mice

As described above, eosinophils were observed within 24 h following installation of MWCNT in WT mice (Figure 2B). Because eosinophil influx was not expected in the

airways, the time course of eosinophil recruitment was confirmed with a second assay, EPO. WT and IL-1R$^{-/-}$ mice instilled with DM or HN-MWCNT underwent WLL at 24 h or 28 days post exposure (Figure 6A). Differential cell counts confirmed the previous results (Figure 2B), a marked influx of eosinophils from HN-MWCNT in the WLL of the WT mice compared to DM-treated mice. Although not statistically significant, the presence of eosinophils was detected in the lungs of the IL-1R$^{-/-}$ mice after exposure to HN-MWCNT. Somewhat unexpectedly, but consistent with the R_L results, at 28 days HN-MWCNT significantly increased eosinophil recruitment in the IL-1R$^{-/-}$ mice, while no eosinophils were detected in either HN-MWCNT or DM-treated WT mice at 28 days. The time course of eosinophil infiltration was further supported with measurements of EPO (Figure 6B). In the WT mice, there was an early spike in the recruitment of eosinophils with HN-MWCNT exposure that peaked around 1 day then rapidly decreased, but not back to pretreatment values. In contrast, the recruitment is slow, but continuous in IL-1R$^{-/-}$ mice treated with HN-MWCNT.

Discussion

The results from this study demonstrated that MWCNT exposure induced IL-1β production within 24 h and was accompanied by an acute inflammatory response that included not only neutrophils, but also eosinophils (Figures 2 and 3). Furthermore, the acute response was also accompanied by an increase in lung resistance (Figure 5). Measurements of lung lavage cytokines indicated that in addition to IL-1β there were increases in TNF-α, IL-6 and MCP-1 protein levels following MWCNT exposure. To evaluate the role of the NLRP3 inflammasome in this model, these studies were repeated in mice lacking the IL-1R. The results revealed that loss of IL-1R signalling could reduce the acute inflammatory response, demonstrated by diminished influx of inflammatory cells and lung resistance in response to MWCNT exposure. Furthermore, although the increase in IL-1β, IL-6 and TNF-α still occurred in IL-1R$^{-/-}$ mice, MCP-1 was significantly blocked suggesting that the increase in MCP-1 was downstream of IL-1β (Figure 3). Together, these results suggest that inhibition of IL-1β would reduce the acute inflammatory response to MWCNT exposure, consistent with models of monosodium urate, and diesel exhaust particles induced NLRP3 activation (Provoost et al. 2011; So et al. 2007).

IL-1β is a potent pro-inflammatory cytokine that is crucial for host response to infection and injury (Dinarello 1996). It is of particular interest because of previous findings that demonstrated an association between exposure to TiO_2 nanobelts and increased IL-1β production, *in vitro* and *in vivo* (Hamilton et al. 2009). Furthermore, IL-1β production has been associated with mediation of diverse sterile inflammatory responses, autoimmune disorders and fibrosis (Cassel et al. 2008; Maynard et al. 2006; Rock et al. 2010). Our hypothesis was that blocking IL-1β would cause a reduced pulmonary inflammatory response in mice exposed to MWCNT. The inflammatory response in WT mice treated with MWCNT included elevated numbers of total cells, specifically, a significant influx of neutrophils and eosinophils at 24 h. Indeed, in contrast to the WT mice, IL-1R$^{-/-}$ mice exposed to MWCNT resulted in a reduced pulmonary inflammatory response.

An acute inflammatory response in the lung is often initiated by AM through its innate immune activity orchestrating subsequent infiltration of neutrophils by production of IL-1, IL-6 and TNFα (Dinarello 1996). Although AM uptake of MWCNT was clearly observed in both WT and IL-$1^{-/-}$ mice, the influx of neutrophils was blocked in IL-$1^{-/-}$ mice (Figure 2), supporting the important role of IL-1β in initiating the inflammatory response. Similarly, other studies using IL-$1R^{-/-}$ mice demonstrated inhibition of the neutrophilic response, both to pathogens and cellular injury (Miller et al. 2006; Provoost et al. 2011). The loss of the neutrophilic response in IL-$1R^{-/-}$ mice could have important implications. As the first line of defence and the most abundant immune cell in humans, neutrophils react to danger signals from infected or injured tissue, where they release antimicrobial factors and reactive oxygen species to eliminate pathogens and sanitise injured tissues (Kessenbrock et al. 2011). In MWCNT-induced pulmonary fibrosis, the absence of neutrophils and subsequent lack of phagocytosis could result in prolonged MWCNT retention in the tissue, which may in part account for the increased fibrosis observed in the IL-$1R^{-/-}$ mouse compared to the WT (Figures 2 and 4). These findings are consistent with a previous report where depletion of blood leukocytes caused increased fibrosis in the lungs of mice exposure to quartz (Henderson et al. 1991).

Consistent with the proposed role of IL-1β, there was a diminished amount of total cells at 28 days recruited to the lungs of the mice null for IL-1R signalling in comparison to the WT mice. Neutrophil counts were negligible in WT mice and continued to be absent in $IL1R^{-/-}$ mice at the 28-day time point (data not shown). These results suggest that, the absence of neutrophils was likely a result of decreased production of chemotactic factor MCP-1 (Figure 3) and that the release of MCP-1 was downstream of IL-1 signalling. Additionally, although the levels were at or below the level of detection for the assay (data not shown at 24 h) production of keratinocyte-derived chemokine (Guran et al. 2009) was decreased in the lavage fluid of IL-$1R^{-/-}$ mice, compared to the WT mice. Similar results were reported using IL-$1R^{-/-}$ mice and the IL-1Ra, which inhibited induction of MCP-1 and KC by DEP (Provoost et al. 2011).

To investigate the role of IL-1R signalling in the chronic inflammatory response to MWCNT, WLL and lung tissue as well as lung resistance were assessed in WT and IL-$1R^{-/-}$ mice 28 days after a single exposure to MWCNT. The results demonstrated an inflammatory response with the presence of granuloma-like foci and collagen-rich fibrotic tissue in the WT mice consistent with previous studies (Porter et al. 2010; Ryman-Rasmussen et al. 2009; Wang et al. 2011). However, lung fibrosis and granuloma-like lesions were exacerbated in the IL-$1R^{-/-}$ compared to the WT mouse. Consistent with the increased pathological lesions, there was an increased inflammatory cell component in the lung lavage fluid that included eosinophils and increased lung resistance in the IL-$1R^{-/-}$ mice that had essentially disappeared in the WT mice by 28 days. These findings are in contrast with the results from genetic variability studies or using the IL-1R antagonist Anakinra (Barlo et al. 2011; So et al. 2007). To the best of our knowledge, this is the first investigation of the effects of fibrosis induced by MWCNT in the IL-$1R^{-/-}$ mouse model. The increased chronic inflammatory response and pathology in the IL-$1R^{-/-}$ model could be due to increased persistence of MWCNT in the lung with the absence of neutrophil clearance. Alternatively, the effects of other signals (e.g., IL-33) may be enhanced in the

absence of IL-1β signalling (Beamer et al. 2012). Although TNF-α has been associated with lung fibrosis (Gao et al. 2011; Liu et al. 1998; Liu & Brody 2001), it was not detected in the WLLF of either WT or IL1R$^{-/-}$ mice at 28 days post exposure to MWCNT(data not shown), therefore does not appear to play a role in the development of MWCNT-induced pulmonary fibrosis in the IL1R$^{-/-}$ mouse.

Elevated numbers of eosinophils have been observed in WLL of sensitised mice exposed to SWCNT and MWCNT in models of allergic airway inflammation (Inoue et al. 2009; Nygaard et al. 2009). However, to the best of our knowledge, this is the first study to report the presence of eosinophils in the lavage fluid of C57BL/6 mice after 24 h of exposure to MWCNT. These results (Figures 2 and 6) demonstrate that eosinophils were recruited to the lungs as a result of exposure to MWCNT. Additionally, the number of eosinophils was greatly diminished in the acute response in mice deficient for IL-1R signalling. IL-5, IL-13 and eotaxin levels were slightly elevated in the particle-exposed WT mice compared to vehicle. However, no differences in these mediators were observed between WT and IL-1R$^{-/-}$ mice (unpublished data). Unexpectedly, after 28 days, the presence of eosinophils as well as EPO levels continued to be elevated in the WLL IL-1R$^{-/-}$ compared to the WT mice (Figure 6). These results suggest that IL-1R signalling could mediate regulatory events for eosinophilia clearance.

In this study, airway hyperreactivity was evaluated in WT and IL-1R$^{-/-}$ mice at 24 h and 28 days post installation to MWCNT. R_L was significantly increased in WT mice, but not in IL-1R$^{-/-}$ mice at 24 h post installation. However, consistent with the histology and hydroxyproline data at 28 days post exposure to MWCNT, the R_L was significantly elevated in the mice null for IL-1R compared the WT mice. Taken together, the results suggest that MWCNT exposure produces combined inflammatory infiltrates (AMs, neutrophils and eosinophils) and granuloma-like lesions in addition to diminished pulmonary function. Although unknown compensatory mechanisms in the transgenic IL-1R$^{-/-}$ may in part contribute to these observations, these outcomes appear to be dependent on IL-1R signalling in both the acute and chronic responses.

Increased pulmonary fibrosis in IL-1R$^{-/-}$ compared to WT mice was observed in mice infected with *Chlamydia pneumoniae* (He et al. 2010). Similar to our findings using HN-MWCNT (Hamilton et al. 2012a.), *C. pneumoniae* also induces IL-1β by way of lysosomal acidification and cathepsin B release (He et al. 2010). He et al. reported reduced neutrophils and increased infiltrating fibroblasts and fibrosis in the lungs of IL-1R$^{-/-}$ mice compared to WT mice by 6 days post *C. pneumoniae* infection. Furthermore, neutropenia was associated with augmented fibrosis in a mouse model of influenza and may regulate inflammation through secretion of the anti-inflammatory mediator IL-10 (Tate et al. 2009; Zhang et al. 2009). Collectively these reports suggest that the acute response to pathogens and particles is ablated in IL-1R$^{-/-}$ mice, but enhanced in the chronic response suggesting a role for IL-1β signalling in both the initiating and resolution phases of inflammation.

Inexpensive nickel catalyst is being used to generate the large volumes of MWCNT currently in high market demand (Chen et al. 2010). Nickel-associated MWCNT are in use as supercapacitor electrodes in hybrid automobiles and solar panels (Gao et al. 2008; Lang et

al. 2008; Nam et al. 2008). Residues from nickel catalysts used to synthesise MWCNT have been shown to be bioavailable in human epithelium (Liu et al. 2007). In addition, an association was observed with high dose of nickel-containing single-walled carbon nanotubes and increased mortality in a mouse model of exposure (Lam et al. 2004). Our previous studies demonstrated that a correlation exists between the amount of nickel impurity from MWCNT and activation of the NLRP3 inflammasome (IL-1β production) in AM from C57BL/6 mice (data not shown). Furthermore, the increased IL-1β levels were statistically associated with increased presence of granulomatous lung tissue 7 days post exposure to MWCNT. Collectively, the information from the literature supports what our data suggest that the bioactivity of Ni-containing MWCNT can induce NLRP3 inflammasome activation.

In summary, this study has demonstrated that MWCNT induced a severe acute pulmonary inflammation in C57BL/6 mice that was diminished in IL-1R$^{-/-}$ mice in the acute response. Furthermore, although resolution of the acute inflammatory response was observed in the WT mice, a marked increased influx of eosinophils and augmented pulmonary resistance was demonstrated in the IL-1R$^{-/-}$ mice after 28 days of exposure to MWCNT. These data suggest that IL-1R signalling is critical in the clearance of the acute phase inflammatory response to Ni-MWCNT in the lungs of mice and is potentially due to diminished expression of chemotactic factors MCP-1 and KC. Given these results and the projected increase in production and use of MWCNT it is crucial to continue assessment of the toxicological effects of these materials. These studies establish the importance of inflammasome activation in the acute response and resolution from exposure to MWCNT.

Acknowledgments

This work was supported by NIH grants RC2-ES018742, P20-RR017670 and F32 ES019816. The authors thank the core scientists, Mary Buford (Inhalation and Pulmonary Physiology Core), Lou Herritt (Molecular Histology and Fluorescence Imaging Core), Pam Shaw (Fluorescence Cytometry Core), Britten Postma (Animal Core) and Jim Driver (EMTrix) for the shared expertise needed to conduct the experiments described in this manuscript.

References

Barlo NP, Van Moorsel CHM, Korthagen NM, Heron M, Rijkers GT, Ruven HJT, et al. Genetic variability in the IL1RN gene and the balance between interleukin (IL)-1 receptor agonist and IL-1b in idiopathic pulmonary fibrosis. Clin Exp Immunol. 2011; 166:346–351. [PubMed: 22059992]

Beamer CA, Girtsman TA, Seaver BP, Finsaas KJ, Migliaccio CT, Perry VK, et al. IL-33 mediates multi-walled carbon nanotube (MWCNT)-induced airway hyper-reactivity via the mobilization of innate helper cells in the lung. Nanotoxicology. 2012; 6 Epub before print.

Cassel SL, Eisenbarth SC, Iyer SS, Sadler JJ, Colegio OR, Tephly LA, et al. The Nalp3 inflammasome is essential for the development of silicosis. Proc Natl Acad Sci USA. 2008; 105:9035–9040. [PubMed: 18577586]

Chen CH, Su HC, Chuang SC, Yen SJ, Chen YC, Lee YT, et al. Hydrophilic modification of neural microelectrode arrays based on multi-walled carbon nanotubes. Nanotechnology. 2010; 21:485501. [PubMed: 21051797]

Churg A, Zhou S, Wang X, Wang R, Wright JL. The role of interleukin-1beta in murine cigarette smoke-induced emphysema and small airway remodeling. Am J Respir Cell Mol Biol. 2009; 40:482–490. [PubMed: 18931327]

Davis BK, Wen H, Ting JP. The inflammasome NLRs in immunity, inflammation, and associated diseases. Annu Rev Immunol. 2011; 29:707–735. [PubMed: 21219188]

Dinarello C. Biological basis for interleukin-1 in disease. Blood. 1996; 87:2095–2147. [PubMed: 8630372]

Dinarello C. Interleukin-1 in the pathogenisis and treatment of inflamatory diseases. Blood. 2011; 117:3720–3732. [PubMed: 21304099]

Dinarello CA. Immunological and inflammatory functions of the interleukin-1 family. Annu Rev Immunol. 2009; 27:519–550. [PubMed: 19302047]

Dolinay T, Kim YS, Howrylak J, Hunninghake GM, An CH, Fredenburgh L, et al. Inflammasome-regulated cytokines are critical mediators of acute lung injury. Am J Respir Crit Care Med. 2012; 185:1225–1234. [PubMed: 22461369]

Dostert C, Petrilli V, Van Bruggen R, Steele C, Mossman BT, Tschopp J. Innate immune activation through Nalp3 inflammasome sensing of asbestos and silica. Science. 2008; 320:674–677. [PubMed: 18403674]

Foster WM, Walters DM, Longphre M, Macri K, Miller LM. Methodology for the measurement of mucociliary function in the mouse by scintigraphy. J Appl Physiol. 2001; 90:1111–1117. [PubMed: 11181627]

Gao B, Yuan CZ, Su LH, Chen L, Zhang XG. Nickel oxide coated on ultrasonically pretreated carbon naontubes for supercapacitor. J Solid State Electrochem. 2008; 13:1251–1257.

Gao HS, Rong X, Peng D, Chen NF, Bing M, Zhao HB, et al. Cross-talk of the related bioactivity mediators in serum after injection of soluble TNF-alpha receptor on silicosis model of rats. Toxicol Ind Health. 2011; 27:607–616. [PubMed: 21505002]

Guran T, Tolhurst G, Bereket A, Rocha N, Porter K, Turan S, et al. Hypogonadotropic hypogonadism due to a novel missense mutation in the first extracellular loop of the neurokinin B receptor. J Clin Endocrinol Metab. 2009; 94:3633–3639. [PubMed: 19755480]

Hamilton RF, Wu N, Porter D, Buford M, Wolfarth M, Holian A. Particle length-dependent titanium dioxide nanomaterials toxicity and bioactivity. Part Fibre Toxicol. 2009; 6:35. [PubMed: 20043844]

Hamilton R, Buford M, Xiang C, Wu N, Holian A. NLRP3 inflammasome activation in murine alveolar macrophages and related lung pathology is associated with MWCNT nickel contamination. Inhal Toxicol. 2012a in press.

Hamilton R, Girtsman T, Xiang C, Wu N, Holian A. Nickel contamination on MWCNT is related to particle bioactivity but not toxicity in the THP-1 transformed macrophage model. Int J Biomed Nanosci Nanotechnol. 2012b in press.

Harris, P. Carbon nanotubes and related structures: new materials for the 21st Century. Cambridge: Canbridge Unversity Press; 1999.

He X, Mekasha S, Mavrogiorgos N, Fitzgerald KA, Lien E, Ingalls RR. Inflammation and fibrosis during Chlamydia pneumoniae infection is regulated by IL-1 and the NLRP3/ASC inflammasome. J Immunol. 2010; 184:5743–5754. [PubMed: 20393140]

Henderson RF, Harkema JR, Hotchkiss JA, Boehme DS. Effect of blood leucocyte depletion on the inflammatory response of the lung to quartz. Toxicol Appl Pharmacol. 1991; 109:127–136. [PubMed: 2038743]

Hornung V, Bauernfeind F, Halle A, Samstad EO, Kono H, Rock KL, et al. Silica crystals and aluminum salts activate the NALP3 inflammasome through phagosomal destabilization. Nat Immunol. 2008; 9:847–856. [PubMed: 18604214]

Inoue K, Koike E, Yanagisawa R, Hirano S, Nishikawa M, Takano H. Effects of multi-walled carbon nanotubes on a murine allergic airway inflammation model. Toxicol Appl Pharmacol. 2009; 237:306–316. [PubMed: 19371758]

Johnston HJ, Hutchison GR, Christensen FM, Peters S, Hankin S, Aschberger K, et al. A critical review of the biological mechanisms underlying the in vivo and in vitro toxicity of carbon nanotubes: the contribution of physico-chemical characteristics. Nanotoxicology. 2010; 4:207–246. [PubMed: 20795897]

Kang MJ, Choi JM, Kim BH, Lee CM, Cho WK, Choe G, et al. IL-18 induces emphysema and airway and vascular remodeling via IFN-gamma, IL-17A, and IL-13. Am J Respir Crit Care Med. 2012; 185:1205–1217. [PubMed: 22383501]

Kessenbrock K, Dau T, Jenne DE. Tailor-made inflammation: how neutrophil serine proteases modulate the inflammatory response. J Mol Med. 2011; 89:23–28. [PubMed: 20809089]

Lacher SE, Johnson C, Jessop F, Holian A, Migliaccio CT. Murine pulmonary inflammation model: a comparative study of anesthesia and instillation methods. Inhal Toxicol. 2010; 22:77–83. [PubMed: 20017595]

Lam CW, James JT, Mccluskey R, Hunter RL. Pulmonary toxicity of single-wall carbon nanotubes in mice 7 and 90 days after intratracheal instillation. Toxicol Sci. 2004; 77:126–134. [PubMed: 14514958]

Lang JW, Kong LB, Wu WJ, Luo YC, Kang L. Facile approach to prepare loose-packed NiO nano-flakes materials for supercapacitors. Chem Commun (Camb). 2008; 35:4213–4215. [PubMed: 18802533]

Liu X, Gurel V, Morris D, Murray DW, Zhitkovich A, Kane A, et al. Bioavailabilty of nickel in single-wall carbon nanotubes. Adv Mater. 2007; 19:2790–2796.

Liu JY, Brody AR. Increased TGF-beta1 in the lungs of asbestos-exposed rats and mice: reduced expression in TNF-alpha receptor knockout mice. J Environ Pathol Toxicol Oncol. 2001; 20:97–108. [PubMed: 11394717]

Liu JY, Brass DM, Hoyle GW, Brody AR. TNF-alpha receptor knockout mice are protected from the fibroproliferative effects of inhaled asbestos fibers. Am J Pathol. 1998; 153:1839–1847. [PubMed: 9846974]

Martin CR, Kohli P. The emerging field of nanotube biotechnology. Nat Rev Drug Discov. 2003; 2:29–37. [PubMed: 12509757]

Maynard AD, Aitken RJ, Butz T, Colvin V, Donaldson K, Oberdorster G, et al. Safe handling of nanotechnology. Nature. 2006; 444:267–269. [PubMed: 17108940]

Medzhitov R, Preston-Hurlburt P, Kopp E, Stadlen A, Chen C, Ghosh S, et al. MyD88 is an adaptor protein in the hToll/IL-1 receptor family signaling pathways. Mol Cell. 1998; 2:253–258. [PubMed: 9734363]

Miller LS, O'Connell RM, Gutierrez MA, Pietras EM, Shahangian A, Gross CE, et al. MyD88 mediates neutrophil recruitment initiated by IL-1R but not TLR2 activation in immunity against Staphylococcus aureus. Immunity. 2006; 24:79–91. [PubMed: 16413925]

Murphy FA, Schinwald A, Poland CA, Donaldson K. The mechanism of pleural inflammation by long carbon nanotubes: interaction of long fibres with macrophages stimulates them to amplify pro-inflammatory responses in mesothelial cells. Part Fibre Toxicol. 2012; 9:8. [PubMed: 22472194]

Muzio M, Ni J, Feng P, Dixit VM. IRAK (Pelle) family member IRAK-2 and MyD88 as proximal mediators of IL-1 signaling. Science. 1997; 278:1612–1615. [PubMed: 9374458]

Nam SH, Kim YS, Shim HS, Choi SM, Kim HJ, Kim WB. Size controlled nickel oxide nanoparticles on carbon nanotubes for supercapacitor electrode. J Nanosci Nanotechnol. 2008; 8:5427–5432. [PubMed: 19198470]

Nel A, Xia T, Madler L, Li N. Toxic potential of materials at the nanolevel. Science. 2006; 311:622–627. [PubMed: 16456071]

Nygaard UC, Hansen JS, Samuelsen M, Alberg T, Marioara CD, Lovik M. Single-walled and multi-walled carbon nanotubes promote allergic immune responses in mice. Toxicol Sci. 2009; 109:113–123. [PubMed: 19293371]

Palomaki J, Valimaki E, Sund J, Vippola M, Clausen PA, Jensen KA, et al. Long, needle-like carbon nanotubes and asbestos activate the NLRP3 inflammasome through a similar mechanism. ACS Nano. 2011; 5:6861–6870. [PubMed: 21800904]

Porter DW, Hubbs AF, Mercer RR, Wu N, Wolfarth MG, Sriram K, et al. Mouse pulmonary dose- and time course-responses induced by exposure to multi-walled carbon nanotubes. Toxicology. 2010; 269:136–147. [PubMed: 19857541]

Porter D, Sriram K, Wolfarth M, Jefferson A, Schwegler-Berry D, Andrew M, et al. A biocompatible medium for nanoparticle dispersion. Nanotoxicology. 2008; 2:144–154.

Porter D, Wu N, Hubbs A, Mercer R, Funk K, Meng F, et al. Differential mouse pulmonary dose- and time course- responses to titanium dioxide nanospheres and nanobelts. Toxicological Sci. 2012 in press.

Provoost S, Maes T, Pauwels NS, Vanden Berghe T, Vandenabeele P, Lambrecht BN, et al. NLRP3/caspase-1-independent IL-1beta production mediates diesel exhaust particle-induced pulmonary inflammation. J Immunol. 2011; 187:3331–3337. [PubMed: 21844393]

Rock KL, Latz E, Ontiveros F, Kono H. The sterile inflammatory response. Annu Rev Immunol. 2010; 28:321–342. [PubMed: 20307211]

Ryman-Rasmussen JP, Tewksbury EW, Moss OR, Cesta MF, Wong BA, Bonner JC. Inhaled multiwalled carbon nanotubes potentiate airway fibrosis in murine allergic asthma. Am J Respir Cell Mol Biol. 2009; 40:349–358. [PubMed: 18787175]

So A, De Smedt T, Revaz S, Tschopp J. A pilot study of IL-1 inhibition by anakinra in acute gout. Arthritis Res Ther. 2007; 9:R28. [PubMed: 17352828]

Tate MD, Deng YM, Jones JE, Anderson GP, Brooks AG, Reading PC. Neutrophils ameliorate lung injury and the development of severe disease during influenza infection. J Immunol. 2009; 183:7441–7450. [PubMed: 19917678]

Wang X, Katwa P, Podila R, Chen P, Ke PC, Rao AM, et al. Multi-walled carbon nanotube instillation impairs pulmonary function in C57BL/6 mice. Part Fibre Toxicol. 2011; 8:24. [PubMed: 21851604]

Weber A, Wasiliew P, Kracht M. Interleukin-1 (IL-1) pathway. Sci Signal. 2010; 3:cm1. [PubMed: 20086235]

Wells SM, Buford MC, Porter VM, Brunell HL, Bunderson-Schelvan M, Nevin AB, et al. Role of the serotonergic system in reduced pulmonary function after exposure to methamphetamine. Am J Respir Cell Mol Biol. 2010; 42:537–544. [PubMed: 19541843]

Zhang X, Majlessi L, Deriaud E, Leclerc C, Lo-Man R. Coactivation of syk kinase and MyD88 adaptor protein pathways by bacteria promotes regulatory properties of neutrophils. Immunity. 2009; 31:761–771. [PubMed: 19913447]

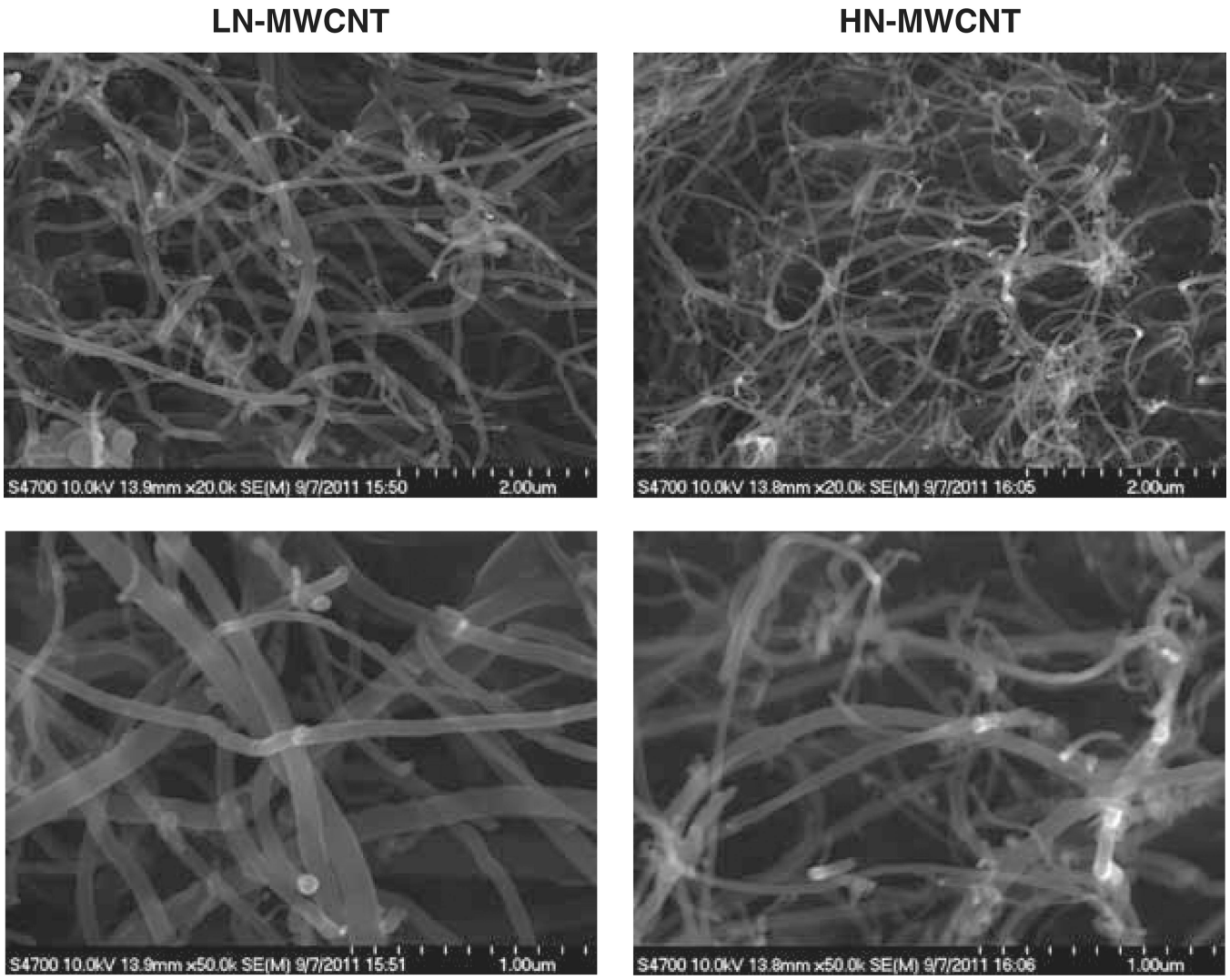

Figure 1.

Characterisation of multi-walled carbon nanotubes was determined using electron microscopy. The images recorded using the scanning electron microscope show LN- and HN-MWCNT. Dry nanoparticle samples were placed on a conductive stick carbon tab on a 12 mm aluminium SEM stub. The stubs were place, uncoated, in a Hitachi S-4700 Field Emission Scanning Electron Microscope and imaged at 10 kv.

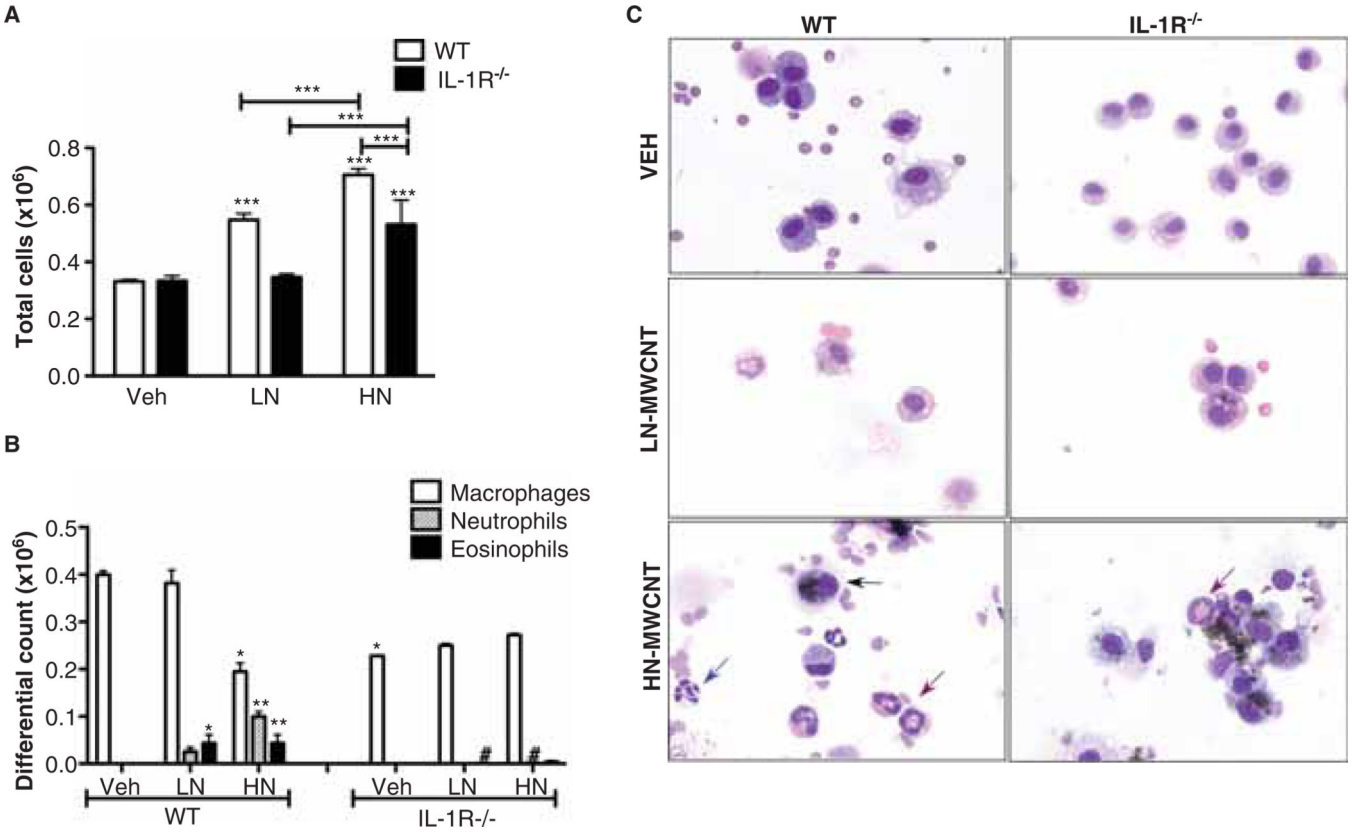

Figure 2.

Total and differential Cell Counts are augmented in mice exposed to MWCNT. WT and IL-1R−/− mice were exposed to LN-MWCNT (2.5% Ni) and HN-MWCNT (5.54% Ni) (50 μg/30 μl) through oropharyngeal aspiration. After 24 h, the lungs were lavaged and total cell counts were determined using the Coulter Z2 particle counter (A). Cells from WLLF (4–10 × 104) were concentrated in PBS by Cytospin (Shandon, Thermo Scientific West Palm Beach, FL) centrifuged for 5 min at 1500 rpm. The slides were processed with Protocol Hema-3 Stain (Fisher Scientific, Houston, TX) (Eosin and Methylene Blue). Differential counts were determined using light microscopy (B and C). Blue and red arrows denote neutrophils and eosinophils, respectively (C). Results are means ± SE ($n = 4$ in each group). *$p < 0.05$, **$p < 0.01$, ***$p < 0.001$, #$p < 0.05$ (vs. WT group).

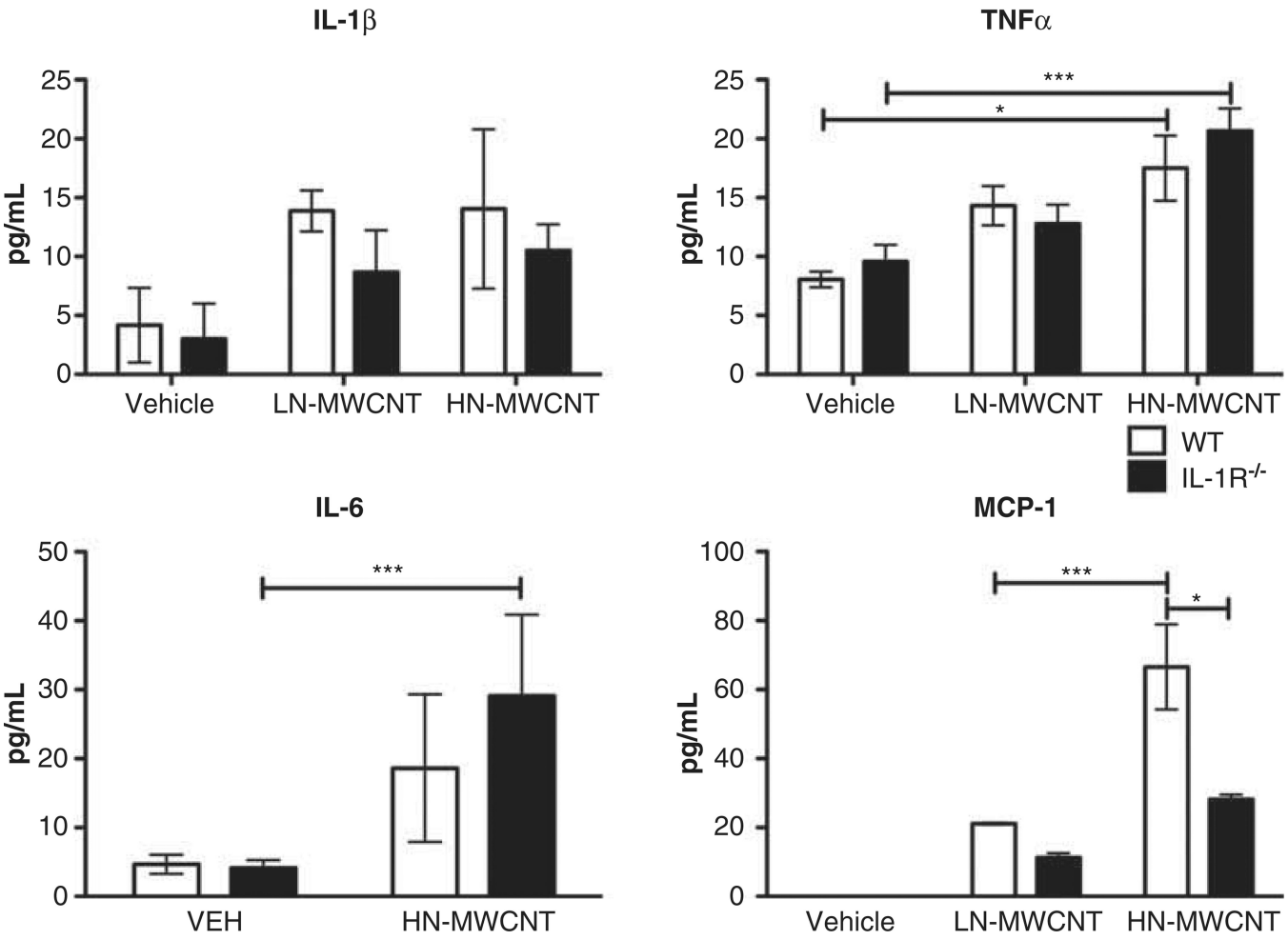

Figure 3.

MWCNT induces chemotactic factors MCP-1 through the IL-1R−/− signalling pathway. WLLF was collected from WT and IL-1R−/− mice 24 h post exposure to LN and HN-MWCNT. The cells were isolated through centrifugation and the supernatants were assayed for IL-1β, IL-6*, TNF-α and MCP-1 by ELISA. *$p < 0.05$, ***$p < 0.001$ versus DM group, #$p < 0.05$ versus WT group. (*Due to shortage of sample, IL-6 assay included only HN-MWCNT WLLF).

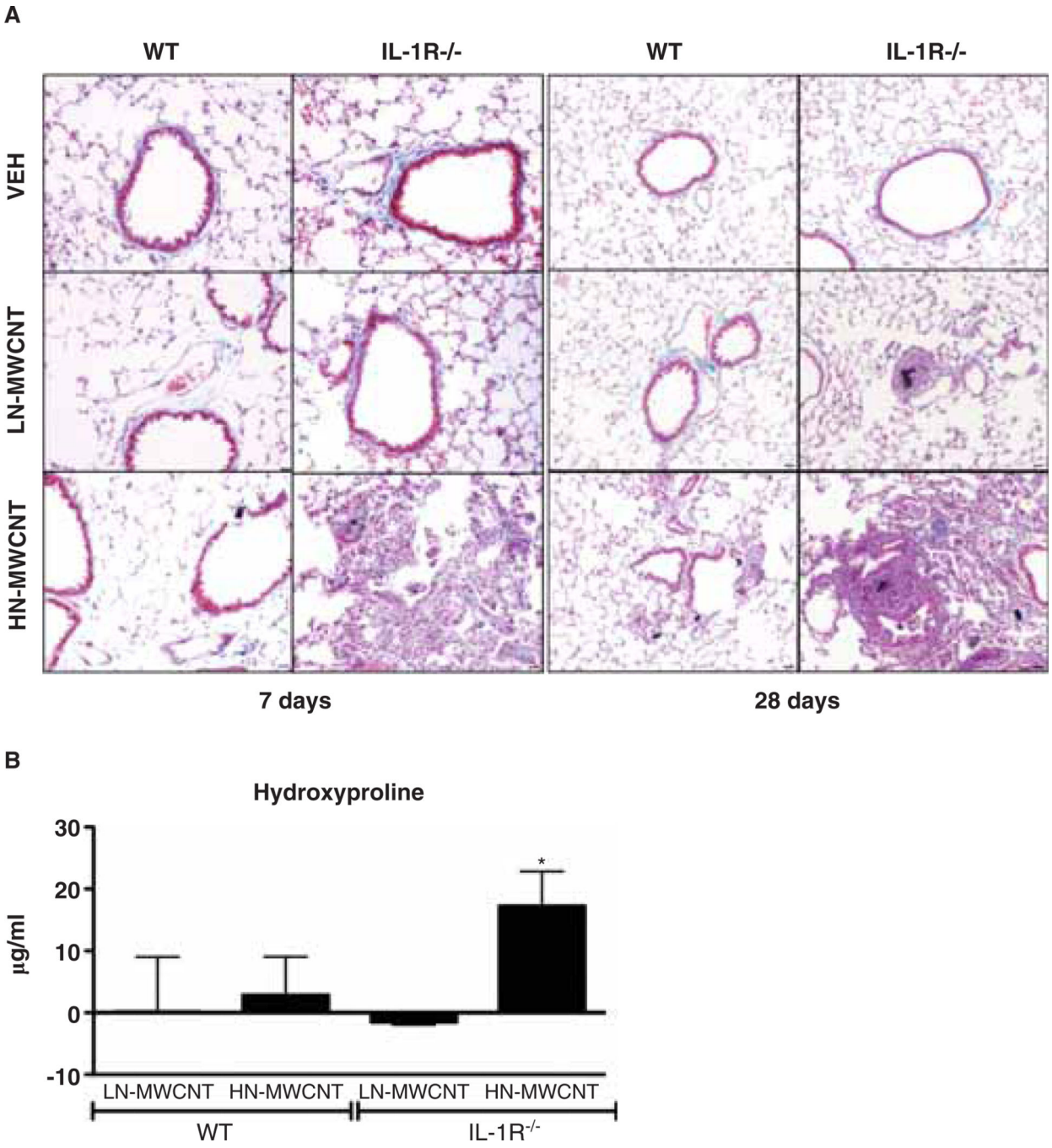

Figure 4.

Collagen deposition is augmented in the lungs of MWCNT-treated mice. Histopathology of lungs of IL-1R−/− mice exposed to MWCNT displays granuloma-like lesions and fibrotic tissue at 7 and 28 days post exposure. The WT or IL-1R−/− mice were euthanised at days 7 and 28 post exposure. After perfusion, the lung tissue from mice instilled with DM only or 50 mg LN- or HN-MWCNT was fixed in paraformaldehyde and imbedded in paraffin. Tissue sections that were stained with Gomori's Trichrome demonstrate collagen-rich granulomas and surrounding fibrotic tissue in lungs of both WT and IL-1R−/− mice exposed

with HN-MWCNT, but not DM (vehicle) control or LN-MWCNT-exposed mice (A). Collagen deposition in the lungs of WT or IL- 1R−/− mice following instillation with LN-, HN-MWCNT was assessed by hydroxyproline assay (n = 3–5 mice/group). The data were normalised by subtracting the mean background from the vehicle-treated mice, from the hydroxyproline levels of the particle-treated animals. Values are means ± SEM; * $p < 0.05$ compared to vehicle controls (B)

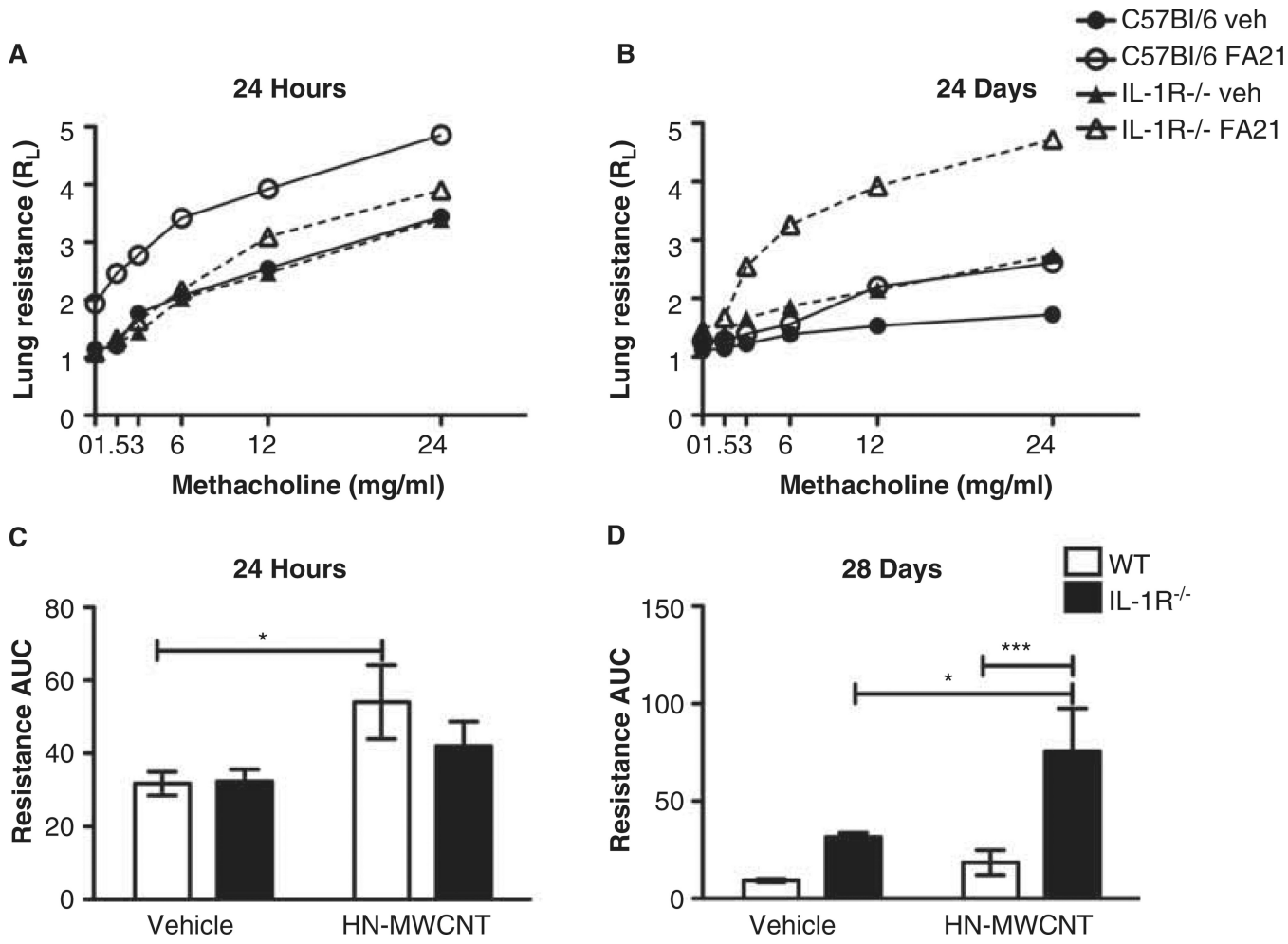

Figure 5.

Pulmonary function at 24 h and 28 days post exposure to HN-MWCNT. Pulmonary function was assessed as a function of increasing methacholine dose in live mice at 24 h or 28 days after exposure to HN-MWCNT (A and B). Transpulmonary resistance (Medzhitov R) was assessed after anaesthetisation and tracheostomy ($n = 6$ for HN-MWCNT, $n = 5$ for vehicle (PBS) control). Two-factor ANOVA and Tukey *post-hoc* statistical analysis were performed to test for statistical significance of the effects of exposure to HN-MWCNT between WT and IL-1R−/− and between each of the vehicle controls. *$p < 0.05$ (C and D).

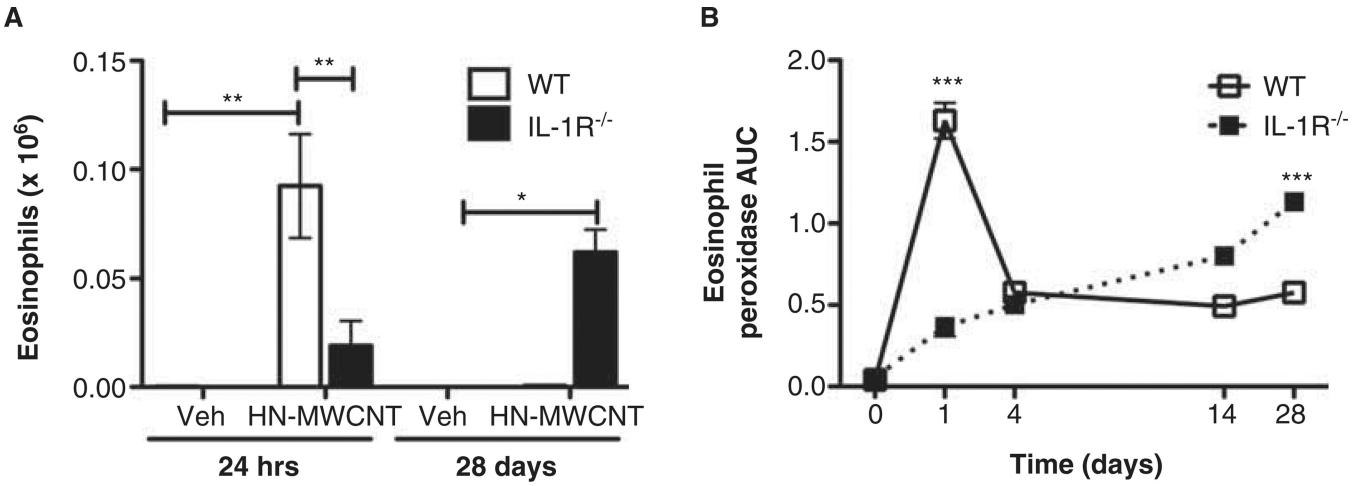

Figure 6.

Acute and chronic influx of eosinophils in to the lungs of mice exposed to HN-MWCNT. WLL was performed on WT and IL-1R−/− mice 24 h or 28 days post exposure to HN-MWCT. The total cell and differential counts were performed. After 24 h of exposure, a significant influx of eosinophils was detected in the WLLF of WT mice in comparison to the vehicle control (*$p > 0.05$). After 28 days of exposure IL-1R−/− mice have demonstrate a prolonged eosinophilia compared to the vehicle-treated mice and the HN-MWCNT WT mice (*$p > 0.05$ vs. vehicle; #$p > 0.05$ vs. WT mouse) (A). EPO levels were assayed to verify the presence of eosinophils in the lavage fluid collected from the lungs of the mice exposed to HN-MWCNT (B).

Table I

MWCNT Characterisation Data.

Supplier	ID	Fe	Co	Ni	Mo	Purity	Diameter (mean)	Length (range)	Zeta Potential	Suspended Agglomeration State
		% of mass					nm	pm	mV	nm
MK Impex	Low Ni-MWCNT	0.054	0.013	2.54	0.1	97.3	33	5–15	−11.3	682
SunNano	High Ni-MWCNT	0.441	0.008	5.54	0	94	27	5–15	−12	429

Descriptive Data for Low Nickel and High Nickel-MWCNT (LN-MWCNT and HN-MWCNT) investigated in this study. Median particle diameter and length range of dry material are as described in the methods section. The MWCNT was suspended in DM and sonicated as in the methods section for the agglomeration characterisation. The length of suspended agglomerated particles is unattainable at present time.